Journal of Psychiatric Research 194 (2026) 303–311

Contents lists available at ScienceDirect

Journal of Psychiatric Research

journal homepage: www.elsevier.com/locate/jpsychires

Implicit social animations lead to distinct changes of dopaminergic, corticostriatal and thalamocortical functional connectivity in schizophrenia and bipolar disorder

Ricardo Martins [a,1], João Valente Duarte [a,b,1], Nuno Madeira [a,d,e], António Macedo [a,d,e], Miguel Castelo-Branco [a,c,*]

[a] Coimbra Institute for Biomedical Imaging and Translational Research (CIBIT), Institute for Nuclear Sciences Applied to Health (ICNAS), University of Coimbra, Portugal
[b] Champalimaud Clinical and Research Centre, Champalimaud Foundation, Lisbon, Portugal
[c] Institute for Physiology, Faculty of Medicine, University of Coimbra, Portugal
[d] Institute of Psychological Medicine, Faculty of Medicine, University of Coimbra, Portugal
[e] Department of Psychiatry, Centro Hospitalar e Universitário de Coimbra (CHUC), Portugal

ARTICLE INFO

Keywords:
Schizophrenia
Bipolar disorder
Theory of mind
Functional connectivity
Social cognition
Dopaminergic
Limbic

ABSTRACT

Objective: Theory of mind (ToM) is a central pillar of social cognition and crucial for effective social interactions. Impairment in ToM is a major predictor of global functioning in schizophrenia (SCZ) and bipolar disorder (BPD). Based on the hypothesis that subcortical and reward circuit functional connectivity is distinct in SCZ and BPD and can be better revealed using ToM task-based approaches, we tested whether functional connectivity patterns of cortico-subcortical networks are a discriminative feature of these disorders.

Methods: We conducted a cross-sectional study (n = 60) to investigate the modulation of task-induced functional connectivity in SCZ (n = 20), BPD (n = 20), and healthy controls (n = 20) during implicit ToM processing with a visual paradigm leading to the interpretation of social meaning based on simple geometric figures with implied social content. Functional connectivity was estimated using generalized psychophysiological analysis of functional magnetic resonance imaging data.

Results: We found unique connectivity patterns in SCZ and BPD within subcortical loops. The SCZ group exhibited specifically disrupted connectivity in corticostriatal and thalamocortical pathways involving ToM and the mesolimbic pathways. A single common pattern of aberrant connectivity in BPD and SCZ occurred between the VTA and dorsal striatum, suggesting increased midbrain-striatal (actor-critic) connectivity in both disorders.

Conclusions: The unique patterns of altered connectivity in SCZ (imbalance between striatothalamic and thalamocortical connectivity), and BPD, while sharing a common pattern of increase between VTA and dorsal striatum, may represent candidate biomarkers of pathophysiological significance, or as biological targets for validating differential therapeutic neuromodulation.

1. Introduction

Schizophrenia (SCZ) and bipolar disorder (BPD) are prevalent and debilitating mental disorders that can be challenging to diagnose given their symptomatic heterogeneity and partial overlap (Bhugra et al., 2017). Sharing common genetic risk variations (Psychiatric Genomics Consortium, 2013), their clinical differences raise important questions regarding distinctions on the underlying neurobiology (Craddock et al., 2009). Social cognition impairments (Couture, 2006; Lahera et al., 2012), including ToM (the ability to recognize and understand the mental states of oneself and others), are common in both disorders (Premack and Woodruff, 1978).

While ToM dysfunction has been extensively documented as a prominent predictor of functioning in SCZ (Chung et al., 2014), it was

* Corresponding author. Coimbra Institute for Biomedical Imaging and Translational Research (CIBIT), Institute for Nuclear Sciences Applied to Health (ICNAS), University of Coimbra, Portugal.
E-mail address: mcbranco@fmed.uc.pt (M. Castelo-Branco).
[1] These authors contributed equally to this work.

https://doi.org/10.1016/j.jpsychires.2026.01.016
Received 1 June 2025; Received in revised form 14 December 2025; Accepted 8 January 2026
Available online 8 January 2026

less studied in BPD (Mitchell and Young, 2016), despite recognition as a key domain of functioning in this condition (Lahera et al., 2012). The extent of ToM impairment in SCZ and BPD may effect differently on social functioning and the likelihood of successful treatment (Mitchell and Young, 2016). Distinct neural mechanisms may exist for such impairments in each disorder, questioning whether differences are merely dimensional or qualitative.

Meta-analyses of task-based functional magnetic resonance imaging (fMRI) studies that employed ToM paradigms in SCZ or BPD have shown decreased activation in core regions specialized for ToM processing (Bora et al., 2016; Mitchell and Young, 2016; Weng et al., 2022). To our knowledge, a single study of our group compared the neural correlates of ToM processing in SCZ and BPD, using a standard General Linear Model (GLM) approach, revealing contrasting activation patterns in left and right temporoparietal junctions between clinical groups (Madeira et al., 2021), challenging the dimensional perspective.

It is reasonable to hypothesize that the degree and/or type of ToM dysfunction might relate with disrupted connectivity patterns in relevant networks. Indeed, a recent imaging study in healthy individuals (Wang et al., 2021) revealed the specificity of a network of key ToM processing regions; these results were replicated in an electrocorticography study in epilepsy (Tan et al., 2022). However, an open question remains whether ToM processing relates with cortico-subcortical connectivity changes in dopaminergic corticostriatal and thalamic loops in SCZ and BPD, thereby defining a qualitative dichotomy. Previous studies showed disruptions in functional connectivity (FC) of various circuits in SCZ or BPD (Bellani et al., 2020; Bi et al., 2022; Dobri et al., 2022; Jimenez et al., 2019; Yoon et al., 2021), supporting a common overall pattern of connectivity dysfunction centered on frontal and limbic areas (Dobri et al., 2022). However, these apparently similar patterns didn't address subcortical connectivity. Few studies have specifically examined FC during ToM tasks in these populations (Martin et al., 2016; Schilbach et al., 2016; Willert et al., 2015), and, to our knowledge, no studies have directly compared ToM-related brain FC patterns between SCZ and BPD patients. Additionally, task-based fMRI paradigms may capture more behaviourally relevant information than resting-state FC (Zhao et al., 2023).

Following previous work (Madeira et al., 2021), focused on the TPJ and revealing contrasting activation patterns in SCZ and BPD using a social perception decision task, and driven by theoretical neuroanatomical and neurochemical structured models of ToM, we hypothesized that key subcortical structures related to social cognition, in particular reward and limbic regions, could present distinctive neural dynamics and functional interactions in SCZ vs. BPD during tasks requiring domain-general social judgment. Our hypothesis is that SCZ and BPD will present distinct global cognitive ToM processing in this decision task requiring interpretation of social interaction content across multiple types of geometric animations. Using multiple types of animations allowed to generalize performance assessment. To test this, we employed generalized psychophysiological interaction (gPPI) analysis of fMRI data to investigate subcortical FC of implicit ToM processing in SCZ and BPD patients, as well as healthy controls, during a visual ToM task requiring social interpretation of agents' interactions and the inference of meaning from the motion trajectories of simple animated geometric figures. We focused on parts of a neuroanatomical ToM model (Abu-Akel and Shamay-Tsoory, 2011) specifically addressing interactions between regions typically associated with ToM, and other areas within cortico-striatal-thalamo-cortical circuits and dopaminergic pathways. This model proposes that generating representations of mental states begins at posterior brain regions, namely the TPJ, yet how this relates with dopaminergic and subcortical processing in these disorders remains unknown. Thus, this ToM network model includes limbic-paralimbic and frontal regions underlying affective and cognitive ToM, and the anterior cingulate cortex (ACC) responsible for regulating their interaction. In addition, the model incorporates regions of the cortico-striatal-thalamo-cortical circuits (pallidum and thalamus) and dopaminergic pathways (ventral tegmental area - VTA, and substantia nigra - SN). This approach explores shared and distinct aberrant neural processes underlying ToM processing in SCZ and BPD, with a focus on cortico-subcortical pathways and whether they represent categorical or dimensional distinctions, further detailing the biological processes underlying discriminative features of these psychiatric conditions.

2. Methods

2.1. Participants

Right-handed patients with BPD (n = 20) and SCZ (n = 20) matched for age (range 18–54 years), gender, and education were recruited from the outpatient setting of a large tertiary hospital. Handedness was assessed through the Edinburgh Handedness Inventory (Espírito-Santo et al., 2017). All patients had an International Classification of Diseases 10th Revision diagnosis of BPD or SCZ confirmed through a direct interview by an experienced psychiatrist and medical records reviewing. Inclusion criteria were unchanged medication for at least 3 months, and clinical stability verified as: sustained euthymia in BPD patients (Brief Psychiatric Rating Scale - BPRS (Caldas de Almeida et al., 1996) mania and depression items $\leq$1); in SCZ, Positive and Negative Symptoms Scale for Schizophrenia - PANSS (Kay et al., 1987) score variation <10 %. Exclusion criteria included neurological or other medical conditions (e.g. epilepsy, head trauma), comorbid alcohol or other drugs abuse/dependence, and MRI contraindications. Twenty right-handed healthy controls (CTR) verifying the same exclusion criteria and matched for age, gender and education were recruited from hospital and faculty workers and their relatives; only subjects with no personal or first-degree family history of psychiatric disorders were included. The study was approved by the Ethics Commission of the Faculty of Medicine of the University of Coimbra (ref. CE-010/2014), and conducted in accordance with the Declaration of Helsinki. All participants provided written informed consent before participating in the study. Participants completed an extensive neuropsychological assessment protocol, previously outlined in our earlier work (Madeira et al., 2021).

2.2. Imaging data acquisition and experimental design

Neuroimaging data were collected with a Siemens Magnetom TIM Trio 3T scanner (Siemens, Munich, Germany) with a phased array 12-channel birdcage head coil. Briefly, functional images were acquired with whole-brain coverage with TR = 2000ms, TE = 39ms, flip angle = 90°, and voxel size 3 × 3 × 4mm. Participants were engaged in four runs of a visual task involving ToM animated stimuli with implicit social content (Madeira et al., 2021; Tavares et al., 2008). Visual stimuli were shown inside the MRI scanner bore using an LCD screen (NordicNeuroLab, Bergen, Norway) and through a mirror mounted above participants' eyes. Behavioral responses were collected using two fiber-optical MR-compatible response pads (Cedrus Corporation, San Pedro, USA). An experimental run consisted of 8 trials, each comprising a sequence of baseline, animation movie, jittering, and question blocks. Each experimental run consisted of 8 trials, with each trial comprising a sequence of baseline, animation movie, jittering, and question blocks. Animation movie blocks (14s) were preceded by baseline blocks (12.5–13.5s) and followed by jittering blocks (0–1s). Both baseline and jittering blocks displayed a static, screen-centered fixation circle. The animation movie blocks displayed simple geometric shapes (two circles) interacting on a bidimensional structured scenario (animations available in the supplementary material of Madeira et al., 2021, where we report the GLM analysis). Prior to fMRI scanning, participants were instructed to interpret the animations as representing social interactions between two agents. This design choice was intentional, as our primary goal was to ensure consistent evaluative framework across all conditions. There were four different animation categories: affiliative (friendly social interaction), antagonistic (hostile social interaction), indifferent

(non-interacting social movements), linear (non-interacting rectilinear movements). All animation categories employed the same type of bidimensional structured scenario; the only element that varied across categories was the agents' movement pattern, which defined the specific animation category that had to be inferred by the participant in this decision task. Participants could not anticipate the category of a given trial based on overall changes in the scenario. Instead, to achieve a perceptual interpretation they had to attend to the circles' movements, progressively integrate the information, apply the same evaluative framework, and then classify the interaction during the question block (eg: affiliative and antagonistic trials unfold progressively from initially quasi-linear or indifferent movements and contain ambiguity that is only resolved later in the video; linear animations can be interpreted as agents walking or running at a constant pace). Each animation in the study was unique, ensuring comparable novelty and processing demands across trials. During question blocks, an interrogative sentence was presented for 8.5s, asking participants to classify the emotional valence of the social interactions depicted in the preceding animations as positive (affiliative), negative (antagonistic), or neutral (indifferent or linear). Representative videos of the animation categories are provided in the Supplementary Materials of our previous work (Madeira et al., 2021). These animations were originally developed and validated in a previous study (Tavares et al., 2008). Although behavioural performance on the ToM task is not reported in detail in the present work, these results have already been presented and discussed in our previous study (Madeira et al., 2021), and are consistent with the validation reported by Tavares et al. (2008). In that work, CTR group demonstrated very high accuracy in classifying the animations. Two SCZ participants performed two and three experimental runs, respectively, due to fatigue. Complete information regarding MRI data acquisition and experimental design can be found in the supplementary material.

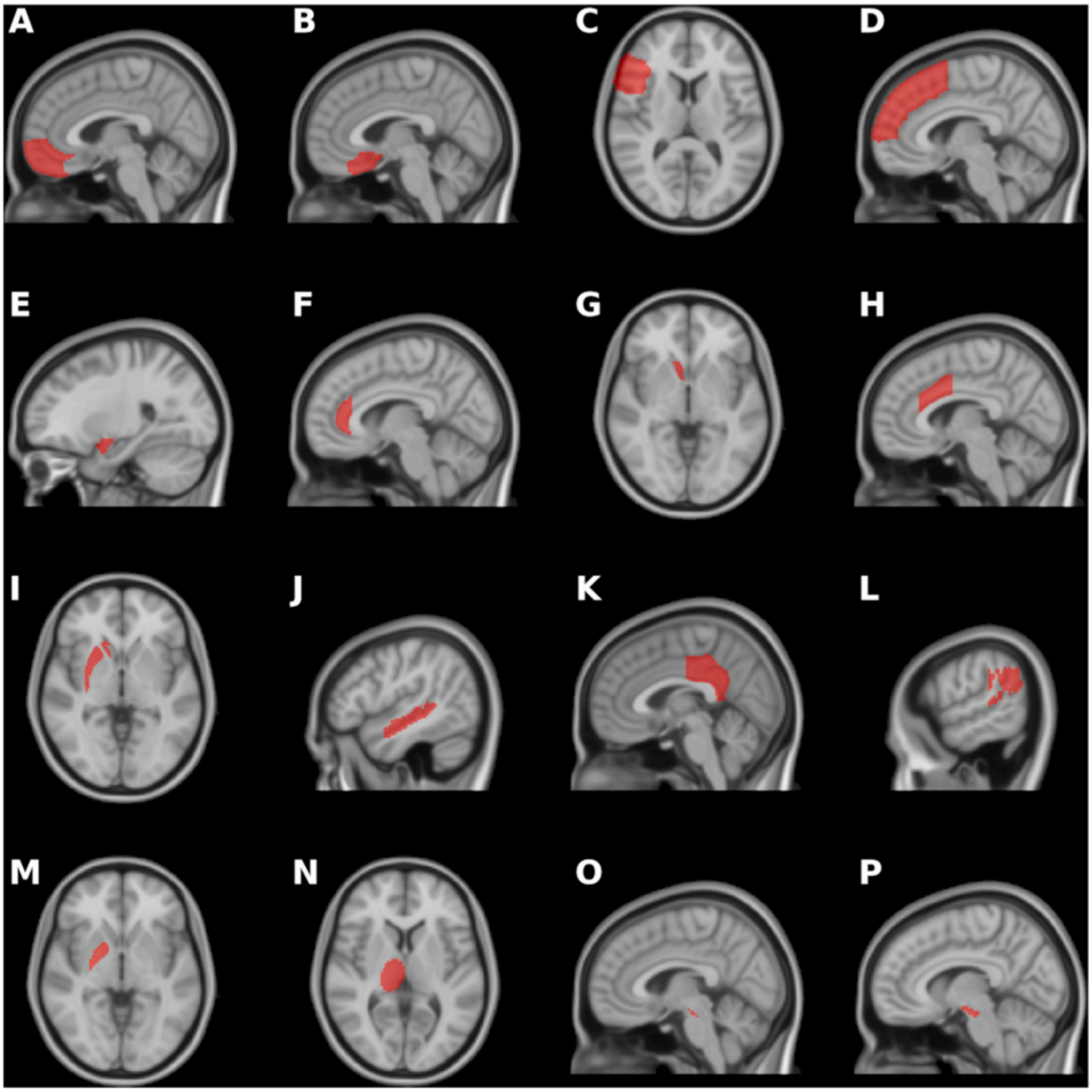

Fig. 1. – Representation of brain areas on a Montreal Neurological Institute (MNI) template for ROI-to-ROI functional connectivity analysis within the ToM network, displaying only a single slice of the right hemisphere ROIs. A) vmPFC, ventromedial prefrontal cortex; B) OFC, orbitofrontal cortex; C) IFG, inferior frontal gyrus; D) dmPFC, dorsomedial prefrontal cortex;; E) Amy, amygdala; F) vACC, ventral anterior cingulate cortex; G) vStri, ventral striatum; H) dACC, dorsal anterior cingulate cortex; I) dStri, dorsal striatum; J) STS, superior temporal sulcus; K) PCC, posterior cingulate cortex; L) TPJ, temporoparietal junction; M) Pal, pallidum; N) Thal, thalamus; O) VTA, ventral tegmental area; P) SN, substantia nigra.

2.3. Functional connectivity analysis

A set of seed regions-of-interest (ROI) was used to assess ROI-to-ROI task-related functional connectivity with a generalized psychophysiological interaction (gPPI) analysis of fMRI data (McLaren et al., 2012), which was implemented in CONN toolbox (Nieto-Castanon, 2020) (version 20a; MATLAB R2019b; Ubuntu 18.04.6 LTS) following the procedures described below.

2.3.1. ROI selection

The ROI-to-ROI functional connectivity analysis was conducted using a group of 32 ROIs (16 brain areas in each hemisphere), defining the neuroanatomical and neurochemical model of ToM presented in (Abu-Akel and Shamay-Tsoory, 2011). This approach and model have been used in previous works to investigate fMRI connectivity dysfunctions in clinical populations between neural areas dedicated to ToM (Isernia et al., 2022). Our study's analysis did not focus on cortico-cortical connections and homotopic inter-hemispheric connections between the ROIs presented in Fig. 1 of the ToM processing model.

The ROIs spanned cortical and sub-cortical regions and were derived from several gold-standard atlas, including Brainnetome (Fan et al., 2016; Carlén, 2017), AAL3 (Rolls et al., 2020), FSL Harvard-Oxford subcortical (Desikan et al., 2006; Bush et al., 2000), FSL Oxford-GSK-Imanov (Tziortzi et al., 2011), AICHA (Joliot et al., 2015), Mars TPJ Parcellation (Mars et al., 2012). The ROIs are displayed in a template brain in Fig. 1, and the full list of ROIs with the source atlas is presented in Table S1 of the supplementary material.

2.3.2. Generalized psychophysiological interaction analysis

Imaging data pre-processing and cleaning were performed following CONN's default pre-processing pipelines for functional and anatomical data (Nieto-Castanon, 2020). A comprehensive description of imaging data pre-processing and denoising is provided in the supplementary material.

The CONN's ROI-to-ROI generalized psychophysiological interaction (gPPI) analysis is a method that uses multiple regression to assess the level of task-modulated functional connectivity between pairs of ROIs (a seed ROI and a target ROI). This pairwise computation was performed for each participant's possible combinations (seed and target) of ROIs within the above-mentioned ToM model, using the signal of all the functional runs.

For the first-level analysis, each regression model included the following predictors: a predictor defined by the seed ROI BOLD time-series, the main physiological factor; a box-car predictor convolved with the canonical hemodynamic response function for each experimental condition (animation movie: affiliative, antagonistic, indifferent, linear; jittering; question: affiliative, antagonistic, indifferent, linear), the main psychological factors; and predictors corresponding to interaction terms (PPI terms) specified as the product of the main physiological factor and the main psychological factors. For a given pair of seed and target ROI, the output of the gPPI analysis is defined as the regression coefficients (β) associated with the model's interaction terms (PPI terms). This work is focused only on the analysis of the β related with the PPI terms of the animation movies, which, for the sake of simplicity, were labelled as $\beta_{ppi\_affiliative}$, $\beta_{ppi\_antagonistic}$, $\beta_{PPI\_indifferent}$, β_{PPI_linear}. These beta values describe the task-related modulation of functional connectivity, thus, are a measure of connectivity change during the corresponding animation movies category blocks compared to the baseline blocks. A positive or negative β expresses an increase or decrease, respectively, in connectivity during the corresponding animation movies blocks compared to the baseline blocks.

The CONN toolbox applies a General Linear Model (GLM) framework for all second-level (group-level) analyses of functional connectivity. For each ROI-to-ROI connection, β values for each condition and subject were entered into the GLM, together with a between-subjects factor coding the group (CTR, SCZ, BPD). Group differences in task-modulated functional connectivity were assessed in the CONN toolbox using a between-subjects contrast ("any-differences," F-test), while a between-conditions contrast ("average") was specified to capture overall effects across animation categories. This GLM configuration is equivalent to a one-way ANOVA, with β_{ppi_movie} as the dependent variable and group as the independent variable. The β_{ppi_movie} corresponds to the average of the condition-specific values ($\beta_{ppi\_affiliative}$, $\beta_{ppi\_antagonistic}$, $\beta_{ppi\_indifferent}$, β_{ppi_linear}) for each subject. Our approach was designed to assess global group differences in generalized ToM processing scenario, irrespective of animation category. ROI-to-ROI connections that reached significance at $p < 0.01$ (uncorrected) were further tested for group × animation category interactions (threshold $p < 0.05$, uncorrected). No significant interactions were observed, and all connections were maintained for the post hoc tests. Post hoc between-group comparisons were conducted with the Tukey-Kramer correction for multiple comparisons, with significance set at $p < 0.05$ (corrected) using MATLAB Statistics and Machine Learning Toolbox.

In addition, MATLAB was used to conduct receiver-operating-characteristic (ROC) analyses for each pair of groups, with the area under the curve (AUC) calculated from the β_{ppi_movie} values of each statistically significant connection to assess their discriminatory power and complement the group differences analysis.

3. Results

The distribution of estimates of task-induced changes in connectivity during ToM stimulation blocks (β_{ppi_movie}) across subjects of each group is presented in Figs. 2 and 3 for each ROI-to-ROI connection within the ToM network model showing a statistically significant main effect of group (F-test in the one-way ANOVA). A comprehensive summary of statistics for connections with a significant main effect of group, together with the corresponding post-hoc pairwise tests, is presented in Table 2. Table 2 also includes the omega-squared values (ω^2) and the absolute Hedges' g values, which are measures of the effect size for the one-way ANOVA results and the post-hoc pairwise group comparisons, respectively. These effect-size measures provide a clearer characterization of the magnitude and practical relevance of the observed effects.

The statistically significant ROI-to-ROI connections were depicted in two separate figures for clarity. Fig. 2 highlights connections related to key reward brain regions (VTA, SN, vStri) in dopaminergic signalling during ToM processing. Fig. 3, on the other hand, highlights connections primarily within cortico-dorsal striatal-thalamo-cortical circuits.

We can clearly observe in the circular plots, that the functional connectivity patterns between brain regions of ToM processing neuroanatomical model are altered differently in the SCZ and BPD during this ToM task, including increases and decreases in connectivity. We can observe a distinctive task-dependent alteration of functional connectivity specific to SCZ that deviates from the control participants and BPD.

No statistically significant differences were found between the functional connectivity profiles of BPD and CTR, except for increased connectivity between VTA and dorsal striatum, which is also observed in SCZ, and reduced functional connectivity between the SN and PCC, a posterior core region of ToM processing, specific to BPD.

We found increased thalamo cortical connectivity regarding the temporoparietal junction (TPJ) and reduced thalamo striatal connectivity in the ventral striatum (vStri), both specific to SCZ. Overall, in addition to the thalamus, which is a central hub relaying information across different domains and levels of ToM processing circuits, the brain regions with dysfunctional connections in the SCZ group are not only related with affective value reward functions (OFC, vStri, vmPFC) but also with cognitive functions (dACC, dStri, dmPFC) and core posterior regions of the ToM processing (TPJ), as well. This indicates a specific but complex pattern of functional connectivity dysregulation in SCZ.

The results of ROC and AUC analysis are presented in Table S3 of the supplementary material. Overall, we found that the individual β_{ppi_movie}

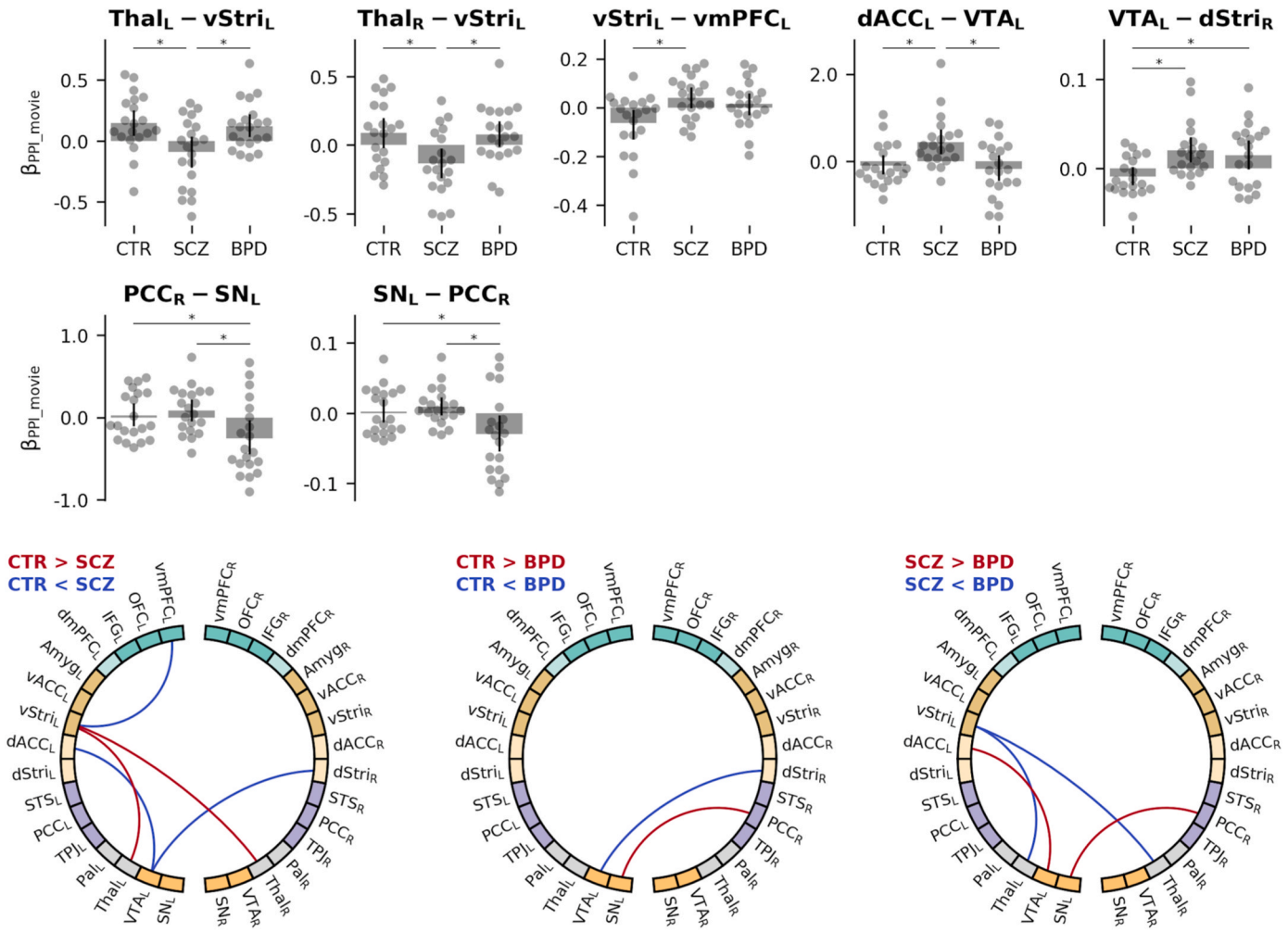

Fig. 2. Functional connectivity engaging key brain regions (VTA, SN, vStri) related to dopaminergic signalling in ToM processing. Top panel: Distribution of estimates of task-induced changes in connectivity during ToM stimulation blocks (β_{ppi_movie}) across subjects of each group, for the statistically significant ROI-to-ROI connections with a main effect of group ($p_{uncorrected} < 0.01$). An asterisk indicates statistically significant pairwise posthoc tests (*), with $p_{Tukey} < 0.05$. The bar depicts the mean, and the whiskers show the 95 % confidence interval of the mean. Bottom panel: Circular plots display ROI-to-ROI connections with statistically significant differences in post-hoc pairwise group comparisons (CTR vs SCZ, CTR vs BPD, and SCZ vs BPD). The direction of the difference in task-induced connectivity changes between groups is highlighted in red or blue connections on the circular plots. The ROI nodes are color-coded to indicate frontal affective (dark green) and cognitive (light green) regions; limbic/paralimbic affective (dark brown) and cognitive (light brown) regions; the posterior core of the theory of mind regions (purple), the thalamic-pallidal regions (grey), and the midbrain nuclei (orange). (For interpretation of the references to color in this figure legend, the reader is referred to the Web version of this article.)

values could differentiate between SCZ and CTR, as well as SCZ vs. BPD, across various connections. Future work should expand on the scope and results of this study by designing and validating candidate connectivity biomarkers using robust machine learning methodologies.

4. Discussion

The main findings of this study are that using a visual social animation task we observed altered connectivity in SCZ manifested as an imbalance across corticostriatal and thalamocortical connectivity, in particular concerning reward pathways. Specifically, we found altered connectivity in processing streams involving ToM and the mesolimbic and mesocortical pathways. The functional connectivity pattern seems to be fundamentally distinct in schizophrenia and bipolar disorder during implicit theory of mind processing. Both disorders showed increase midbrain-striatal (actor-critic) connectivity. Guided by an actor-critic model, we have previously found evidence that the dorsal striatum and the ventral tegmental area may function as the actor and the critic, respectively (Araújo et al., 2024). Midbrain regions such as the VTA play a relevant roles by sending dopaminergic learning signals to the basal ganglia for behavioural adjustment, and this seems to be relevant both for SCZ and BPD.

The identification of this qualitative dichotomy is a unique finding in the field, as no previous study has assessed the task-related modulation of functional connectivity during theory of mind processing and its impact in dopaminergic and corticostriatal and thalamocortical pathways simultaneously in a single sample of schizophrenia and bipolar disorder individuals matched for age, gender, education, and several other clinical and neuropsychological variables (see Table 1 and our previous work (Madeira et al., 2021)). Previous research has primarily focused on the association between clinical symptoms and functional connectivity patterns in ToM networks in resting-state (Jimenez et al., 2019; Bellani et al., 2020; Bi et al., 2022; Yoon et al., 2021), or alternatively, on the study of functional connectivity dysfunctions using a range of different ToM paradigms, but always in separate samples of schizophrenia or bipolar disorder (Bi et al., 2022; Yoon et al., 2021; Schilbach et al., 2016; Martin et al., 2016; Willert et al., 2015). By contrast, our novel findings were observed in well-characterized clinical groups with relatively short illness duration, both of which underwent identical assessments of social neurocognition and were administered

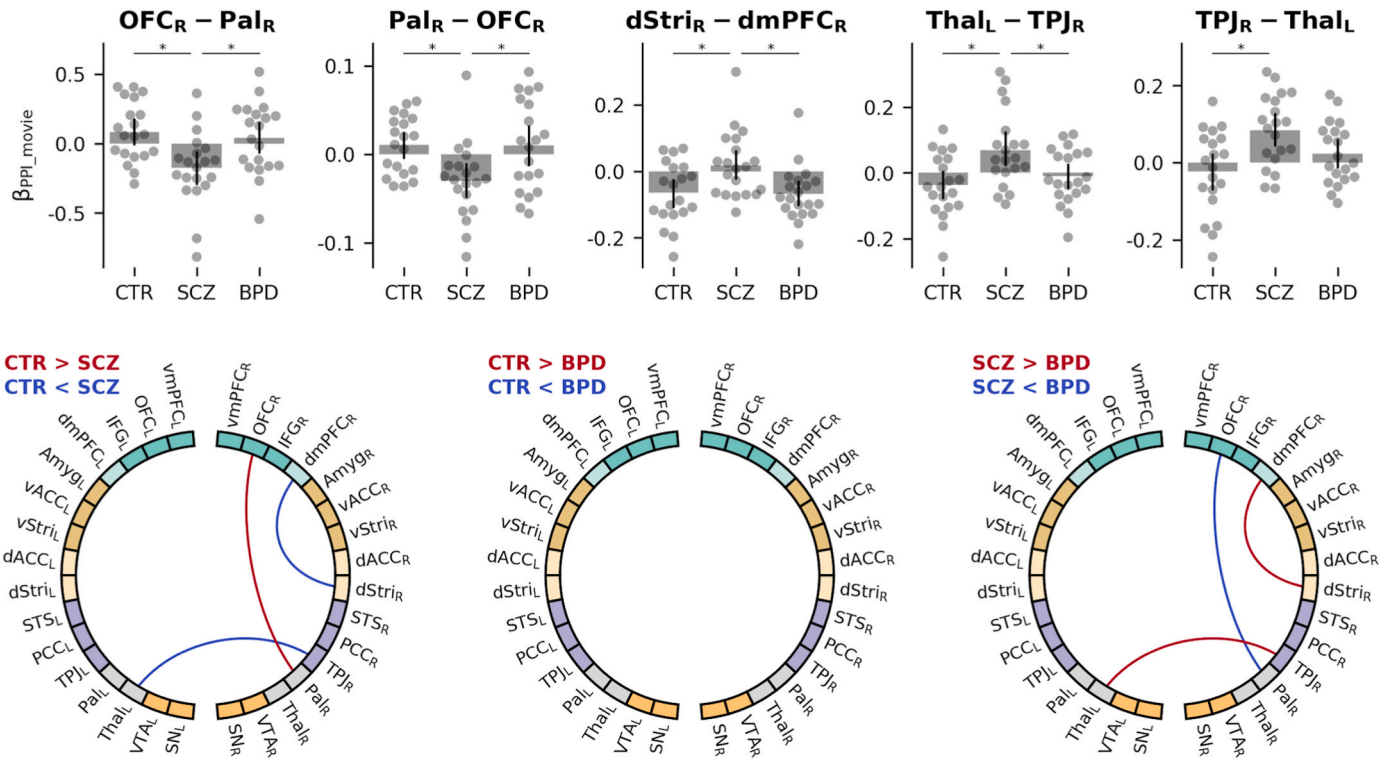

Fig. 3. Functional connectivity within cortico-dorsal striatal-thalamo-cortical circuits during Theory of Mind (ToM) processing. Top panel: Distribution of estimates of task-induced changes in connectivity during ToM stimulation blocks (β_{ppi_movie}) across subjects of each group, for the statistically significant ROI-to-ROI connections with a main effect of group ($p_{uncorrected} < 0.01$). An asterisk indicates statistically significant pairwise posthoc tests (*), with $p_{Tukey} < 0.05$. The bar depicts the mean, and the whiskers show the 95 % confidence interval of the mean. Bottom panel: Circular plots display ROI-to-ROI connections with statistically significant differences in post-hoc pairwise group comparisons (CTR vs SCZ, CTR vs BPD, and SCZ vs BPD). The direction of the difference in task-induced connectivity changes between groups is highlighted in red or blue connections on the circular plots. The ROI nodes are color-coded to indicate frontal affective (dark green) and cognitive (light green) regions; limbic/paralimbic affective (dark brown) and cognitive (light brown) regions; the posterior core of the theory of mind regions (purple), the thalamic-pallidal regions (grey), and the midbrain nuclei (orange). (For interpretation of the references to color in this figure legend, the reader is referred to the Web version of this article.)

Table 1
Demographic and psychopathologic sample characteristics.

	Schizophrenia	Bipolar Disorder	Healthy Controls	Test statistics	
Gender, male/female	13/7	13/7	13/7	N/A	N/A
Age, years (mean ± SD)	31.5 ± 10.3;	31.6 ± 10.0	31.5 ± 10.3	F = 0.001[a]	p = 0.992
Education, years (mean ± SD)	13.6 ± 3.7	13.85 ± 2.64	14.9 ± 4.52	F = 0.756[a]	p = 0.474
Age of onset, years (mean ± SD; range)	25.6 ± 6.9; 18-41	26.5 ± 8.8; 16-50	N/A	t = −0.276[b]	p = 0.784
Duration of illness, years (mean ± SD; range)	6.0 ± 7.9; 1-17	5.2 ± 4.3; 1-16	N/A	t = −0.297[b]	p = 0.769
Number of lifetime admissions (mean; range)	1.25; 0-7	1.25; 0-4	N/A	t = −0.000[b]	p = 1.000
Antipsychotics, CPZE	380.0 (50–1600)	160.8 (0–1066)	N/A	t = 2.226[b]	p = 0.032*
Psychotropic treatment, DDD (range)	0.96 (0.20–3.50)	0.81 (0.00–2.00)	N/A	t = 0.755[b]	p = 0.455
History of psychosis, n (%)	20 (100 %)	16 (80 %)	N/A	χ2 = 4.444[c]	p = 0.106
History of substance use, n (%)	5 (25 %)	7 (35 %)	N/A	χ2 = 0.476[c]	p = 0.731
History of suicidal behaviors, n (%)	4 (20 %)	4 (20 %)	N/A	χ2 = 0.000[c]	p = 1.000

BPD – bipolar disorder; CPZE - chlorpromazine equivalents; CTR – controls; DDD – defined daily dose; SCZ – schizophrenia; SD – standard deviation.
[a] ANOVA.
[b] t Student test.
[c] Chi square.

the same fMRI paradigms. Furthermore, the behavioural analysis of the ToM fMRI task showed that the three groups (SCZ, BPD, and CTR) had matched task performance in both correct response rates and mean response times across stimuli (Madeira et al., 2021).

The distinct task-dependent alteration in functional connectivity within the SCZ group compared to the CTR and BPD groups involved multiple regions across the frontal (OFC, dmPFC, vmPFC), limbic-paralimbic (dStri, vStri, dACC) and posterior core regions of the ToM network. In addition to disruptions in functional connections involving the PFC, OFC, ACC, TPJ and striatum, we observed that in SCZ, subcortical regions such as the VTA, pallidum, and thalamus were also involved in connections with abnormal connectivity. This suggests a general multi-level dysregulation in the cortico-striatal-thalamo-cortical circuits involved in ToM processing (Fig. 3) and partially modulated by the dopaminergic systems stemming from the midbrain (VTA) and vStri (Fig. 2). The ToM processing neuroanatomical model (Abu-Akel and Shamay-Tsoory, 2011) integrated evidence from the classical cortico-striatal-thalamo-cortical model (Sabaroedin et al., 2022; Peters et al., 2016) which established feedback loops between the ventral and dorsal striatum, and the ventral and dorsal regions of the PFC,

Table 2
ROI-to-ROI connections with statistically significant group differences in task-induced changes in connectivity (β_{ppi_movie}) during ToM stimulation blocks.

Connection		Group Main Effect[a)]			Post hoc[b)]					
					CTR vs. SCZ		CTR vs. BPD		SCZ vs. BPD	
Source	*Target*	*F(2,57)*	P_{uncor}	ω^2	P_{Tukey}	| *g* |	P_{Tukey}	| *g* |	P_{Tukey}	| *g* |
$Thal_L$	$vStri_L$	6.009	0.004	0.143	**0.007**	**0.910**	0.938	0.117	**0.018**	**0.862**
$Thal_R$	$vStri_L$	5.923	0.005	0.141	**0.009**	**0.918**	0.981	0.059	**0.015**	**0.909**
$vStri_L$	$vmPFC_L$	5.230	0.009	0.124	**0.008**	**0.916**	0.061	0.668	0.713	0.285
$dACC_L$	VTA_L	6.543	0.003	0.156	**0.015**	**0.953**	0.905	0.135	**0.004**	**0.960**
VTA_L	$dStri_R$	5.554	0.006	0.132	**0.008**	**1.095**	**0.035**	**0.801**	0.834	0.160
PCC_R	SN_L	5.357	0.007	0.127	0.854	0.202	**0.037**	**0.723**	**0.009**	**0.885**
SN_L	PCC_R	5.008	0.009	0.118	0.858	0.226	**0.046**	**0.664**	**0.012**	**0.846**
OFC_R	Pal_R	6.486	0.003	0.155	**0.004**	**1.064**	0.834	0.186	**0.019**	**0.819**
Pal_R	OFC_R	5.815	0.005	0.138	**0.011**	**1.036**	0.997	0.021	**0.014**	**0.824**
$dStri_R$	$dmPFC_R$	5.664	0.006	0.135	**0.016**	**0.845**	0.993	0.036	**0.012**	**0.926**
$Thal_L$	TPJ_R	6.300	0.003	0.150	**0.003**	**0.988**	0.679	0.289	**0.034**	**0.778**
TPJ_R	$Thal_L$	6.377	0.003	0.152	**0.002**	**1.034**	0.277	0.475	0.118	0.681

[a)] Statistical significance threshold $p_{uncorrected} < 0.01$.
[b)] The results of the pairwise post-hoc tests that are statistically significant (corrected $p_{Tukey} < 0.05$) are highlighted in bold.

respectively, passing through the pallidum and thalamus to connect back to the cortex. We also considered the VTA as a core source of dopaminergic projections to the ventral striatum (mesolimbic pathway), PFC (mesocortical pathway), and dorsal striatum. Previous studies (Ungless, 2004; Bromberg-Martin et al., 2010; Horvitz, 2000; Knolle et al., 2018) indicate that midbrain dopaminergic neurons (VTA, SN) respond to various forms of saliency (novelty, emotional salience, and rareness/deviance), all in the absence of explicit rewarding feedback, not just to reward and error-signalling paradigms. In our study, unique implicit social cognition animations were presented to enhance novelty and motivation, which could have favoured the recruitment of these brain regions. On the other hand, regions associated with dopaminergic circuitry that predict others' actions and update mental state representations (Schultz et al., 1997), incorporating both externally and internally generated information, are likely to be involved in ToM processing dysfunctions (Abu-Akel and Shamay-Tsoory, 2011). Or study required participants to progressively gather perceptual evidence as the two dynamic agents interacted and updated their emotional representations (four distinct categories, 14 s per animation) to accurately report the emotional valence of social behaviors depicted in the animations. A previous study showed that the dopaminergic levels in midbrain nuclei predict brain activity as a function of the reward value of social interactions and in response to emotional salience (Jabbi et al., 2013). Our results support the evidence (Knolle et al., 2018) of abnormal functional connectivity in SCZ between regions involved in general salience processing, and not only in explicit reward-related processes. The observed widespread dysregulation of functional connectivity across multiple domains of the ToM model in the SCZ group also highlights the conclusions of a recent review (Robison et al., 2020), which demonstrates that SCZ does not arise from simple and compartmentalized dysfunctions (eg: reward, cognition). Instead, it results from a synergistic dysregulation where each subnetwork continually affects the others in a bidirectional manner.

While our study specifically examines the functional connectivity during implicit affective ToM stimulus blocks, participants were also tasked with classifying the emotional valence of social behaviours depicted in animations in the subsequent task blocks. These results support the idea of synergistic dysregulation, revealing the interdependence of emotional and cognitive mechanisms. Specifically, emotional representations and affective valuation can work as influence signals in decision-making processes (Abu-Akel and Shamay-Tsoory, 2011). As proposed in the ToM processing model, the ACC works as a hub and establishes the interconnection between the affective and cognitive processing streams. The SCZ showed an increased functional connectivity between dACC and VTA, which represents the core mesocortical pathway. The dACC has been implicated in cognitive functions such as response selection, attention-for-action, and error detection, and is also a part of the limbic system. The connection between dACC and VTA has been investigated as a potential biomarker for monitoring treatment response in patients with SCZ (Hadley et al., 2014), namely its role in regulating motivated behaviour by influencing the drive to pursue rewards (Aberg et al., 2020).

While in SCZ, the functional connectivity between dACC and VTA shows an increase compared to the CTR and BPD groups, other connections, such as between OFC and Pal, exhibit a decrease. Thalamic connections, which integrate and transmit information across various domains and stages of ToM processing, also exhibit a mixed pattern: increased connectivity with the TPJ but decreased connectivity with the vStri. This results of mixed functional connectivity dysfunctions, whether increased or decreased, are consistent with previous findings in SCZ (Sabaroedin et al., 2022).

In contrast to SCZ, BPD did not exhibit a generalized dysregulation across the circuits implicated in the ToM or reward processing model, except for the increased connectivity between VTA and dorsal striatum (actor-critic pathway), disfunction shared with SCZ, and a specific reduction in functional connectivity between SN and PCC, which is a posterior core region of the ToM processing model (Abu-Akel and Shamay-Tsoory, 2011). This is interesting because of the recent identification of a direct cortico-nigral pathway. Research on BPD patients has been limited and has yielded inconsistent findings regarding dopamine circuitry (Ashok et al., 2017). Some studies have found no differences compared to controls, while others have suggested dopaminergic dysregulation.

The specific differences in SCZ and BPD regarding connections involving posterior core regions of ToM processing, the TPJ and PCC, respectively, highlight distinct dysfunctions at different stages of ToM pathways. The TPJ plays a primary role in representing mental states, while the PCC transmits these representations to limbic and paralimbic regions for emotional processing and integration with sensory input (Abu-Akel and Shamay-Tsoory, 2011). Both regions also play a crucial role in assigning agency to mental states in ToM processing (Abu-Akel and Shamay-Tsoory, 2011), and our results suggest that disruptions in these processes may differ between SCZ and BPD.

Notably, although the SCZ and BPD groups differed in their exposure to antipsychotic medication (Table 1), a linear correlation between the CPZE score and β_{PPI_movie} was assessed for all the connections with a main group effect of alterations of connectivity, and no significant correlations were found in either group (see Table S2 in the supplementary

material), suggesting that medication is not playing a relevant role in this context.

Regarding common patterns, we found increased connectivity in the actor critic system, involving the VTA and dorsal striatum. The actor-critic framework explains trial-and-error learning whereby an "actor" learns a policy and selects actions, while a "critic" estimates the reward value of such actions and generates a prediction error (Araújo et al., 2024, 2025). Such reinforcement learning mechanisms seem to be critical for adaptive goal-directed behaviour during complex tasks involving social cognition. The observed pattern may reflect a common compensatory pattern across SCZ and BPD.

In conclusion, our findings suggest that specific functional dynamic patterns across thalamocortical and corticostriatal pathways, personalized for distinct domain-general ToM dysfunctions in SCZ and BPD patients, could identify candidate targets for differential therapeutic neuromodulation, guiding non-pharmacological intervention on social dysfunction and addressing daily life handicaps faced by these patients (Zhang et al., 2022).

A potential limitation of our study is the moderate sample size (n = 60). However, the sample was carefully designed with close matching between groups in relevant domains, and we investigated group differences using a task-based ToM paradigm. In addition, the statistical corrections applied were not the most conservative, which should be considered when interpreting the findings. Nevertheless, the observed connectivity differences within the ToM network between well-matched patient groups and controls using this ToM paradigm, suggest stable, trait-like features with potential clinical relevance. The ROC analysis further supports these findings and points to the feasibility of larger machine learning studies to validate candidate functional connectivity biomarkers using our ToM paradigm and ROI framework.

Although the present study focused on domain-general ToM functional connectivity disruptions, using a social perceptual decision task future work should examine whether other types of social interpretation paradigms lead to similar patterns of distinct neural patterns across diagnostic groups, irrespective of the type of condition, as observed here.

CRediT authorship contribution statement

Ricardo Martins: Writing – review & editing, Writing – original draft, Visualization, Software, Formal analysis. **João Valente Duarte:** Writing – review & editing, Writing – original draft, Validation, Investigation, Formal analysis. **Nuno Madeira:** Writing – review & editing, Validation, Conceptualization. **António Macedo:** Writing – review & editing, Validation, Supervision. **Miguel Castelo-Branco:** Writing – review & editing, Validation, Resources, Project administration, Investigation, Funding acquisition, Data curation, Conceptualization.

Funding

This work was supported by the Portuguese Foundation for Science and Technology (FCT), through the projects 'From molecules to man: novel diagnostic imaging tools in neurological and psychiatric disorders' (reference CENTRO-07-ST24-FEDER-00205 and BIGDATIMAGE, CENTRO-01-0145-FEDER-000016), 'MEDPERSYST: Synaptic networks and Personalized Medicine Approaches to Understand Neurobehavioral Diseases Across the Lifespan' (reference SAICTPAC/0010/2015, POCI-01-0145-FEDER-016428), PTDC/PSI-GER/1326/2020, DSAIPA/DS/0041/2020, 2022.02963.PTDC and FCT UIDB/4950/2020 & 2025 and UIDP/4950/2020 & 2025. FCT also funded individual grants to JVD (Individual Scientific Employment Stimulus 2017 - CEECIND/00581/2017) and RM (Institutional Scientific Employment Stimulus 2018 - CEECINST/00041/2018/CP1568/CT0005).

Declaration of competing interest

The authors declare that they have no known competing financial interests or personal relationships that could have appeared to influence the work reported in this paper.

Acknowledgements

We would like to thank the participants for their involvement in this study. We are also very grateful to: Paula Tavares for the ToM visual animation task; Gabriel Costa, Carlos Ferreira and Sónia Afonso for the help with MRI setup and scanning.

Appendix A. Supplementary data

Supplementary data to this article can be found online at https://doi.org/10.1016/j.jpsychires.2026.01.016.

References

Aberg, K.C., Kramer, E.E., Schwartz, S., 2020. Interplay between midbrain and dorsal anterior cingulate regions arbitrates lingering reward effects on memory encoding. Nat. Commun. 11, 1829. https://doi.org/10.1038/s41467-020-15542-z.

Abu-Akel, A., Shamay-Tsoory, S., 2011. Neuroanatomical and neurochemical bases of theory of mind. Neuropsychologia 49, 2971–2984. https://doi.org/10.1016/j.neuropsychologia.2011.07.012.

Araújo, A., Duarte, I.C., Sousa, T., Meneses, S., Pereira, A.T., Robbins, T., Macedo, A., Castelo-Branco, M., 2025. "Actor-critic" dichotomous hyperactivation and hypoconnectivity in obsessive–compulsive disorder. Neuroimage, Clin. 45, 103729. https://doi.org/10.1016/j.nicl.2024.103729.

Araújo, A., Duarte, I.C., Sousa, T., Oliveira, J., Pereira, A.T., Macedo, A., Castelo-Branco, M., 2024. Neural inhibition as implemented by an actor-critic model involves the human dorsal striatum and ventral tegmental area. Sci. Rep. 14, 6363. https://doi.org/10.1038/s41598-024-56161-8.

Ashok, A.H., Marques, T.R., Jauhar, S., Nour, M.M., Goodwin, G.M., Young, A.H., Howes, O.D., 2017. The dopamine hypothesis of bipolar affective disorder: the state of the art and implications for treatment. Mol. Psychiatr. 22, 666–679. https://doi.org/10.1038/mp.2017.16.

Bellani, M., Bontempi, P., Zovetti, N., Gloria Rossetti, M., Perlini, C., Dusi, N., Squarcina, L., Marinelli, V., Zoccatelli, G., Alessandrini, F., Francesca Maria Ciceri, E., Sbarbati, A., Brambilla, P., 2020. Resting state networks activity in euthymic bipolar disorder. Bipolar Disord. 22, 593–601. https://doi.org/10.1111/bdi.12900.

Bhugra, D., Tasman, A., Pathare, S., Priebe, S., Smith, S., Torous, J., Arbuckle, M.R., Langford, A., Alarcón, R.D., Chiu, H.F.K., First, M.B., Kay, J., Sunkel, C., Thapar, A., Udomratn, P., Baingana, F.K., Kestel, D., Ng, R.M.K., Patel, A., De Picker, L., McKenzie, K.J., Moussaoui, D., Muijen, M., Bartlett, P., Davison, S., Exworthy, T., Loza, N., Rose, D., Torales, J., Brown, M., Christensen, H., Firth, J., Keshavan, M., Li, A., Onnela, J.P., Wykes, T., Elkholy, H., Kalra, G., Lovett, K.F., Travis, M.J., Ventriglio, A., 2017. The WPA-lancet psychiatry commission on the future of psychiatry. Lancet Psychiatry 4, 775–818. https://doi.org/10.1016/S2215-0366(17)30333-4.

Bi, B., Che, D., Bai, Y., 2022. Neural network of bipolar disorder: toward integration of neuroimaging and neurocircuit-based treatment strategies. Transl. Psychiatry 12, 143. https://doi.org/10.1038/s41398-022-01917-x.

Bora, E., Bartholomeusz, C., Pantelis, C., 2016. Meta-analysis of theory of mind (ToM) impairment in bipolar disorder. Psychol. Med. 46, 253–264. https://doi.org/10.1017/S0033291715001993.

Bromberg-Martin, E.S., Matsumoto, M., Hikosaka, O., 2010. Dopamine in motivational control: rewarding, aversive, and alerting. Neuron 68, 815–834. https://doi.org/10.1016/j.neuron.2010.11.022.

Bush, G., Luu, P., Posner, M.I., 2000. Cognitive and emotional influences in anterior cingulate cortex. Trends Cognit. Sci. 4, 215–222. https://doi.org/10.1016/S1364-6613(00)01483-2.

Caldas de Almeida, J.M., Gusmão, R., Talina, M., Xavier, M., 1996. Brief Psychiatric Rating Scale (BPRS) Versão Ampliada (4.0) Portuguesa: Escala, Pontos De Ancoragem E Manual De Administração. Psychiatric and Mental Health Department-São Francisco Xavier Hospital, Lisbon.

Carlén, M., 2017. What constitutes the prefrontal cortex? Science 358, 478–482. https://doi.org/10.1126/science.aan8868.

Chung, Y.S., Barch, D., Strube, M., 2014. A meta-analysis of mentalizing impairments in adults with schizophrenia and autism spectrum disorder. Schizophr. Bull. 40, 602–616. https://doi.org/10.1093/schbul/sbt048.

Couture, S.M., 2006. The functional significance of social cognition in schizophrenia: a review. Schizophr. Bull. 32, S44–S63. https://doi.org/10.1093/schbul/sbl029.

Craddock, N., O'Donovan, M.C., Owen, M.J., 2009. Psychosis genetics: modeling the relationship between schizophrenia, bipolar disorder, and mixed (or "schizoaffective") psychoses. Schizophr. Bull. 35, 482–490. https://doi.org/10.1093/schbul/sbp020.

Desikan, R.S., Ségonne, F., Fischl, B., Quinn, B.T., Dickerson, B.C., Blacker, D., Buckner, R.L., Dale, A.M., Maguire, R.P., Hyman, B.T., Albert, M.S., Killiany, R.J., 2006. An automated labeling system for subdividing the human cerebral cortex on MRI scans into gyral based regions of interest. Neuroimage 31, 968–980. https://doi.org/10.1016/j.neuroimage.2006.01.021.

Dobri, M.L., Diaz, A.P., Selvaraj, S., Quevedo, J., Walss-Bass, C., Soares, J.C., Sanches, M., 2022. The limits between schizophrenia and bipolar disorder: what do magnetic resonance findings tell us? Behav. Sci. 12, 78. https://doi.org/10.3390/bs12030078.

Espírito-Santo, H., Pires, C.F., Garcia, I.Q., Daniel, F., Silva, A.G. da, Fazio, R.L., 2017. Preliminary validation of the Portuguese Edinburgh handedness inventory in an adult sample. Appl. Neuropsychol.: Adult 24, 275–287. https://doi.org/10.1080/23279095.2017.1290636.

Fan, L., Li, H., Zhuo, J., Zhang, Y., Wang, J., Chen, L., Yang, Z., Chu, C., Xie, S., Laird, A. R., Fox, P.T., Eickhoff, S.B., Yu, C., Jiang, T., 2016. The human brainnetome atlas: a new brain atlas based on connectional architecture. Cerebr. Cortex 26, 3508–3526. https://doi.org/10.1093/cercor/bhw157.

Hadley, J.A., Nenert, R., Kraguljac, N.V., Bolding, M.S., White, D.M., Skidmore, F.M., Visscher, K.M., Lahti, A.C., 2014. Ventral tegmental area/midbrain functional connectivity and response to antipsychotic medication in schizophrenia. Neuropsychopharmacology 39, 1020–1030. https://doi.org/10.1038/npp.2013.305.

Horvitz, J.C., 2000. Mesolimbocortical and nigrostriatal dopamine responses to salient non-reward events. Neuroscience 96, 651–656. https://doi.org/10.1016/S0306-4522(00)00019-1.

Isernia, S., Pirastru, A., Massaro, D., Rovaris, M., Marchetti, A., Baglio, F., 2022. Resting-state functional brain connectivity for human mentalizing: biobehavioral mechanisms of theory of mind in multiple sclerosis. Soc. Cognit. Affect Neurosci. 17, 579–589. https://doi.org/10.1093/scan/nsab120.

Jabbi, M., Nash, T., Kohn, P., Ianni, A., Rubinstein, D., Holroyd, T., Carver, F.W., Masdeu, J.C., Shane Kippenhan, J., Robinson, S.E., Coppola, R., Berman, K.F., 2013. Midbrain presynaptic dopamine tone predicts sustained and transient neural response to emotional salience in humans: fmri, MEG and FDOPA PET. Mol. Psychiatr. 18, 4–6. https://doi.org/10.1038/mp.2012.12.

Jimenez, A.M., Riedel, P., Lee, J., Reavis, E.A., Green, M.F., 2019. Linking resting-state networks and social cognition in schizophrenia and bipolar disorder. Hum. Brain Mapp. 40, 4703–4715. https://doi.org/10.1002/hbm.24731.

Joliot, M., Jobard, G., Naveau, M., Delcroix, N., Petit, L., Zago, L., Crivello, F., Mellet, E., Mazoyer, B., Tzourio-Mazoyer, N., 2015. AICHA: an atlas of intrinsic connectivity of homotopic areas. J. Neurosci. Methods 254, 46–59. https://doi.org/10.1016/j.jneumeth.2015.07.013.

Kay, S.R., Fiszbein, A., Opler, L.A., 1987. The positive and negative syndrome scale (PANSS) for schizophrenia. Schizophr. Bull. 13, 261–276. https://doi.org/10.1093/schbul/13.2.261.

Knolle, F., Ermakova, A.O., Justicia, A., Fletcher, P.C., Bunzeck, N., Düzel, E., Murray, G. K., 2018. Brain responses to different types of salience in antipsychotic naïve first episode psychosis: an fMRI study. Transl. Psychiatry 8, 196. https://doi.org/10.1038/s41398-018-0250-3.

Lahera, G., Ruiz-Murugarren, S., Iglesias, P., Ruiz-Bennasar, C., Herrería, E., Montes, J. M., Fernández-Liria, A., 2012. Social cognition and global functioning in bipolar disorder. J. Nerv. Ment. Dis. 200, 135–141. https://doi.org/10.1097/NMD.0b013e3182438eae.

Madeira, N., Martins, R., Valente Duarte, J., Costa, G., Macedo, A., Castelo-Branco, M., 2021. A fundamental distinction in early neural processing of implicit social interpretation in schizophrenia and bipolar disorder. Neuroimage, Clin. 32, 102836. https://doi.org/10.1016/j.nicl.2021.102836.

Mars, R.B., Sallet, J., Schuffelgen, U., Jbabdi, S., Toni, I., Rushworth, M.F.S., 2012. Connectivity-based subdivisions of the human right "temporoparietal junction area": evidence for different areas participating in different cortical networks. Cerebr. Cortex 22, 1894–1903. https://doi.org/10.1093/cercor/bhr268.

Martin, A.K., Dzafic, I., Robinson, G.A., Reutens, D., Mowry, B., 2016. Mentalizing in schizophrenia: a multivariate functional MRI study. Neuropsychologia 93, 158–166. https://doi.org/10.1016/j.neuropsychologia.2016.10.013.

McLaren, D.G., Ries, M.L., Xu, G., Johnson, S.C., 2012. A generalized form of context-dependent psychophysiological interactions (gPPI): a comparison to standard approaches. Neuroimage 61, 1277–1286. https://doi.org/10.1016/j.neuroimage.2012.03.068.

Mitchell, R.L.C., Young, A.H., 2016. Theory of mind in bipolar disorder, with comparison to the impairments observed in schizophrenia. Front. Psychiatr. 6. https://doi.org/10.3389/fpsyt.2015.00188.

Nieto-Castanon, A., 2020. Handbook of Functional Connectivity Magnetic Resonance Imaging Methods in CONN. Hilbert Press.

Peters, S.K., Dunlop, K., Downar, J., 2016. Cortico-striatal-thalamic loop circuits of the salience network: a central pathway in psychiatric disease and treatment. Front. Syst. Neurosci. 10. https://doi.org/10.3389/fnsys.2016.00104.

Premack, D., Woodruff, G., 1978. Does the chimpanzee have a theory of mind? Behav. Brain Sci. 1, 515–526. https://doi.org/10.1017/S0140525X00076512.

Psychiatric Genomics Consortium, 2013. Identification of risk loci with shared effects on five major psychiatric disorders: a genome-wide analysis. Lancet 381, 1371–1379. https://doi.org/10.1016/S0140-6736(12)62129-1.

Robison, A.J., Thakkar, K.N., Diwadkar, V.A., 2020. Cognition and reward circuits in schizophrenia: synergistic, not separate. Biol. Psychiatry 87, 204–214. https://doi.org/10.1016/j.biopsych.2019.09.021.

Rolls, E.T., Huang, C.-C., Lin, C.-P., Feng, J., Joliot, M., 2020. Automated anatomical labelling atlas 3. Neuroimage 206, 116189. https://doi.org/10.1016/j.neuroimage.2019.116189.

Sabaroedin, K., Tiego, J., Fornito, A., 2022. Circuit-based approaches to understanding corticostriatothalamic dysfunction across the psychosis continuum. Biol. Psychiatry. https://doi.org/10.1016/j.biopsych.2022.07.017. S0006322322014457.

Schilbach, L., Derntl, B., Aleman, A., Caspers, S., Clos, M., Diederen, K.M.J., Gruber, O., Kogler, L., Liemburg, E.J., Sommer, I.E., Müller, V.I., Cieslik, E.C., Eickhoff, S.B., 2016. Differential patterns of dysconnectivity in mirror neuron and mentalizing networks in schizophrenia. SCHBUL 42, 1135–1148. https://doi.org/10.1093/schbul/sbw015.

Schultz, W., Dayan, P., Montague, P.R., 1997. A neural substrate of prediction and reward. Science 275, 1593–1599. https://doi.org/10.1126/science.275.5306.1593.

Tan, K.M., Daitch, A.L., Pinheiro-Chagas, P., Fox, K.C.R., Parvizi, J., Lieberman, M.D., 2022. Electrocorticographic evidence of a common neurocognitive sequence for mentalizing about the self and others. Nat. Commun. 13, 1919. https://doi.org/10.1038/s41467-022-29510-2.

Tavares, P., Lawrence, A.D., Barnard, P.J., 2008. Paying attention to social meaning: an fMRI study. Cerebr. Cortex 18, 1876–1885. https://doi.org/10.1093/cercor/bhm212.

Tziortzi, A.C., Searle, G.E., Tzimopoulou, S., Salinas, C., Beaver, J.D., Jenkinson, M., Laruelle, M., Rabiner, E.A., Gunn, R.N., 2011. Imaging dopamine receptors in humans with [11C]-(+)-PHNO: dissection of D3 signal and anatomy. Neuroimage 54, 264–277. https://doi.org/10.1016/j.neuroimage.2010.06.044.

Ungless, M.A., 2004. Dopamine: the salient issue. Trends Neurosci. 27, 702–706. https://doi.org/10.1016/j.tins.2004.10.001.

Wang, Y., Metoki, A., Xia, Y., Zang, Y., He, Y., Olson, I.R., 2021. A large-scale structural and functional connectome of social mentalizing. Neuroimage 236, 118115. https://doi.org/10.1016/j.neuroimage.2021.118115.

Weng, Y., Lin, J., Ahorsu, D.K., Tsang, H.W.H., 2022. Neuropathways of theory of mind in schizophrenia: a systematic review and meta-analysis. Neurosci. Biobehav. Rev. 137, 104625. https://doi.org/10.1016/j.neubiorev.2022.104625.

Willert, A., Mohnke, S., Erk, S., Schnell, K., Romanczuk-Seiferth, N., Quinlivan, E., Schreiter, S., Spengler, S., Herold, D., Wackerhagen, C., Romund, L., Garbusow, M., Lett, T., Stamm, T., Adli, M., Heinz, A., Bermpohl, F., Walter, H., 2015. Alterations in neural theory of mind processing in euthymic patients with bipolar disorder and unaffected relatives. Bipolar Disord. 17, 880–891. https://doi.org/10.1111/bdi.12352.

Yoon, S., Kim, T.D., Kim, J., Lyoo, I.K., 2021. Altered functional activity in bipolar disorder: a comprehensive review from a large-scale network perspective. Brain Behav 11. https://doi.org/10.1002/brb3.1953.

Zhang, Y., Li, Y., Wang, Yong-ming, Wang, S., Pu, C.-C., Zhou, S.-Z., Ma, Y.-T., Wang, Yi, Lui, S.S.Y., Yu, X., Chan, R.C.K., 2022. Hub-connected functional connectivity within social brain network weakens the association with real-life social network in schizophrenia patients. Eur. Arch. Psychiatr. Clin. Neurosci. 272, 1033–1043. https://doi.org/10.1007/s00406-021-01344-x.

Zhao, W., Makowski, C., Hagler, D.J., Garavan, H.P., Thompson, W.K., Greene, D.J., Jernigan, T.L., Dale, A.M., 2023. Task fMRI paradigms May capture more behaviorally relevant information than resting-state functional connectivity. Neuroimage 270, 119946. https://doi.org/10.1016/j.neuroimage.2023.119946.